Application of Reverse Time Migration to Complex Imaging Problems

Paul A. Farmer[1], *Ian F.Jones*[2], *Hongbo Zhou*[1], *Robert I. Bloor*[1], *Mike C. Goodwin*[2]

First Break, 2006, v24, p65-73

corresponding author
Ian F. Jones
Tel: +44 1784 497630
ijones@gxt.com

1
GX Technology Corporation
2101 City West Blvd.
Building III, Suite 900,
Houston TX 77042, USA

2
GX Technology EAME
180 High Street, Egham
Surrey TW20 9DY, UK

Application of Reverse Time Migration to Complex Imaging Problems

Paul A. Farmer[1], Ian F.Jones[2] , Hongbo Zhou[1], Robert I. Bloor[1], Mike C. Goodwin[2]
(1) GX Technology Corporation, Houston, (2) GX Technology EAME Ltd

Abstract

Standard shot-based one-way wavefield extrapolation (WE) preSDM techniques image the subsurface by continuing the source and receiver wave-fields for each shot. The imaging condition is invoked by cross correlating these two wave-fields at each depth level, and then summing the contributions from all shots in the aperture to form the image.

One of the assumptions made in using this technique is that the wave-fields travel along the direction of extrapolation only in one direction: downwards for the source wave-field, and upwards for the receiver or scattered wave-field.

In practice, each of these wave-fields will generally travel both up and down when the velocity model is complex, when turning (diving) ray-paths are involved, or when multiples are being generated. In addition, approximations in the extrapolation techniques usually limit the dips present in the final image to less than seventy degrees. Steeper dips, and turning rays are usually imaged using Kirchhoff techniques, but these fail to deliver acceptable images once we have a multi-pathing problem.

One technique which can address all these issues is migration using the two-way wave equation. Here, we have used an anisotropic reverse time migration (RTM) algorithm to achieve this. RTM properly propagates the wave-field through velocity structures of arbitrary complexity, correctly imaging dips greater than 90 degrees. It even has the potential to image with internal multiples when the boundaries responsible for the multiple are present in the model.

Although hitherto considered economically impracticable, recent enhancements to computing capacity, both in terms of CPU speeds and highly efficient hardware infrastructure, have made RTM commercially viable.

Following an historical review of the approximations used in migration, we will show anisotropic RTM examples from the North Sea, outlining the potential benefit of model building and migrating with the full acoustic two-way wave equation.

Historical Background

RTM is perhaps not as well known as other migration algorithms currently in use, and the two-way wave equation is probably less familiar to readers than the one-way simplification. Consequently, we spend some time in the following sections introducing the key concepts involved. For readers already familiar with these concepts, the results section can be referred to directly.

In the early 1990's the limitations on affordable availability of computer power effectively limited migration to the post-stack domain. At the time, a common means of performing post-stack depth migration (postSDM) of 3D seismic data was via the use of frequency domain implicit finite difference (FD) algorithms, first introduced by Claerbout (1976).

To facilitate solution of the 3D wave equation with FD schemes, a technique called 'splitting' was invoked, whereby an independent solution was implemented for the in-line (x) and cross-line (y) directions. This involved separating a double square-root equation (containing the variables x and y) into two independent square root terms one for each of the two variables. It was this splitting, or separation of the x and y components in the data, which resulted in 'numerical anisotropy' -

yielding an impulse response which did not possess the requisite circular x-y section for a constant velocity medium. (The name arises by analogy with physical anisotropy, which results in waves propagating at different velocities in different directions, resulting in a non-spherical wave front at zero-offset).

Each resulting square root term was approximated by a series expansion, the truncation of which led to an incorrect positioning of energy beyond a certain dip in the migrated output. Such series expansion approximations do not have an inherent dip limiting cut-off for the steeper dips where the approximation is no longer valid, but simply erroneously misposition energy beyond this limit. Consequently, a form of noise was introduced appearing as energy travelling at impossibly high velocities for a given propagation angle (thus falling into the evanescent zone of the solution space).

Also, using finite differencing techniques to solve the second-order differential term of the wave equation results in a slight mispositioning of energy as a function of frequency, with respect to the sampling grid of the data. This gives rise to a phenomenon resembling dispersion, in that different frequencies appear to travel at different speeds. During migration a single dipping event will split into a suite of different events each of different frequency content and dip (Diet & Lailly, 1984).

However, the introduction of explicit continuation schemes, free from the FD artefacts, led to steep dip high fidelity postSDM algorithms seen routinely in use by the mid 1990's (Hale, 1991b, Soubaras, 1992).

Integral versus Differential methods

For the most part, these FD and explicit techniques fell into abeyance as postSDM was superseded by Kirchhoff preSDM in the mid to late 1990's, when 3D pre-stack depth imaging became computationally feasible due the appearance of efficient first-arrival travel-time solvers. Furthermore, the ability of Kirchhoff (and other integral methods) to produce limited subsets of the image made industrial application affordable, especially given the fact that we had to apply the imaging methods iteratively to build velocity models. Limitations of the early Kirchhoff migration codes rapidly became evident for complex media, but at that time 3D pre-stack wavefield continuation migration remained unaffordable. So, industrial efforts went towards the improvement of Kirchhoff migration, both in terms of amplitudes and handling different branches of the arrival times.

The terminology that has been used recently is also worth mentioning. Some authors have defined the abbreviation 'WE' to refer to the term 'wave equation' in a way so as to exclude Kirchhoff schemes. However, all migrations are meant to be solutions of the 'wave equation' and so it is imprecise to exclude Kirchhoff schemes from this terminology. Some alternative suggestions were to refer to the alternatives as 'integral' versus 'differential' (or 'extrapolation' or 'continuation') schemes. Here we refer to the differential techniques as wavefield extrapolation (WE), as this abbreviation is interchangeable with the commonly (mis-)used abbreviation for Wave Equation migration.

During the past five years as computer costs have become less of an issue, we have seen a resurgence in one-way WE techniques, but now for the pre-stack domain. Wavefield extrapolation implementations of the one-way scalar wave equation are relatively simple to write compared to a Kirchhoff scheme, but in principle are more costly; the extra cost may be prohibitive if many iterations are needed for construction of the velocity model. With Kirchhoff migration, it is routine to output the data for model update sorted by surface offset (resulting in familiar-looking migrated CRP gathers). For shot domain and other wavefield extrapolation techniques, we require various approximations to produce gathers for velocity analysis.

That being said, with a WE approach we have a better approximation to the true amplitudes of wave propagation, especially in heterogeneous velocity media than with Kirchhoff methods, and the algorithms are readily extendable to two way schemes. Wavefield continuation approaches are best known for their inherent ability to addresses the multi-pathing issue (unlike a Kirchhoff scheme). Recently, we are also seeing renewed interest in the two-way wave equation (Wapenaar, et al, 1987), both with reverse time migration (Whitmore, 1983, Yoon, et al, 2003, Bednar et al, 2003, Farmer, 2006, Zhou, et al, 2006,) and other more approximate wavefield extrapolation techniques (Shan & Biondi, 2004, Zhang et al, 2006).

In Table 1, we summarize the pro's and con's of Kirchhoff (integral) versus wavefield-continuation (WE) approaches.

TABLE 1 (adapted from: Jones & Lambaré, 2003)

Integral Methods	**Differential, Extrapolation or Continuation Methods**
Kirchhoff & Gaussian beam are the best known. Usually implemented in the time domain, but can be in the frequency domain. Distinguishing feature is separation of calculation of travel times from imaging. Thus a subset of the image can be computed without needing to image the entire volume	Finite difference wavefield continuation is the best known, in conjunction with phase shift plus corrections. Each depth slice of the wavefield is computed from the previously computed slice, thus essentially the entire image volume needs to be formed. Dip response is dependent on the order of the expansion used (thus potentially costly)
Strengths: - delivers sub-sets of the imaged volume, including offsets (*thus cost effective for iterative model building*) - good dip response - can yield sub-set of the full two-way solution (turning waves)	**Strengths:** - images all arrivals - simpler amplitude treatment - a full two-way implementation can yield all wave-paths , including prism waves, turning waves, and (perhaps) multiples
Weaknesses - Inherently kinematic - usually only delivers one arrival path - velocity field coarsely sampled for travel time computation, then arrival times interpolated back to seismic spacing - not readily extendible to a full two-way solution	**Weaknesses** - images whole volume (thus costly) - obtaining good dip response is expensive - does not readily produce pre-stack data - thus difficult to achieve cost-effective iterative model building without 'restrictive' assumptions (eg mono-azimuth) - very expensive to invoke a full two-way solution (but can use approximate two pass one-way)

Approximating the Full Elastic Wave Equation

Full solution of the elastic wave equation is not something that we usually set out to achieve. From the standpoint of industrial expediency, we make various simplifying assumptions involving a progression of solutions ranging from the simpler to the more complex. Not surprisingly, this progression has moved in tandem with the increase in available computer power, and development of interactive model update tools (for parameter estimation). An overview of these simplifications, and their relationships to the fundamental equations of elastic wave propagation can be found for

example in the SEG re-print series publication 'Classics of Elastic Wave Theory' (Pelissier, et al, 2006), which charts the development of the equations of motion from the 17th to 20th century. In the more specific context of depth migration, these simplifications are also discussed in the SEG re-print series edition 'Pre-Stack Depth Migration and Velocity Model Building' (Jones, et al, 2006).

Commencing with Stokes' formulation of the Navier equations, which deal with elastic wave propagation in solids, and ending with some computationally tractable algorithms, our first simplification of these equations is to drop the shear terms. Stokes' formulation is a more general rendition of what Cauchy's relations obtain for the isotropic case, Christoffel's do for the anisotropic case, and Navier's do for a formulation with a single elastic constant (Pelissier, et al, 2006).

This progression of industrially implemented solutions over the past two decades can be summarized as:

1. Dropping the shear terms to obtain a P-wave only solution
2. Separating the solution into up and downgoing parts and decoupling them to yield a one-way wave equation solution
3. Avoiding the need to measure vertical pressure derivatives at the surface (a requisite boundary condition for a second order PDE solution), and seeking a solution for near vertical incident angle propagation by adopting a paraxial (parabolic solution)

Perhaps the main difference between RTM and other migration techniques is in the way the propagator handles the data. For the better known one-way migrations, a WE algorithm will take the recorded data, and a band-limited wavelet, and propagate them both through the supplied earth model. The extrapolation step required for this is only dependent on the recorded data's spatial trace spacing and chosen output depth sample rate (and the depth sample rate depends on the maximum frequency desired). For RTM, we are conducting a forward modelling experiment in the time domain, and to extrapolate a given frequency, we typically need about ten samples per wavelength (Alford et al, 1974). If we double the frequency being modelled, we will have twice as many samples per unit length, and as we have three spatial dimensions that a wave propagates in, the cost of modelling will increase in proportion to the cube of the frequency. We must also ensure a similarly fine time sampling rate as well, so the overall cost increases in proportion to the fourth power of frequency.

An intermediate route to addressing turning wave energy using a one-way WE scheme is to employ the two-pass one-way scheme. In this approach we first downward continue using one of the square root solutions, (and saving the evanescent wavefield that corresponds to the complex square root solution). We then migrate the saved complex root terms reversing the direction of propagation. With such a scheme (using roughly double the CPU time of a one-way scheme), we can image turning waves and prism waves (double bounce arrivals: Bernitsas et al, 1997, Cavalca & Lailly, 2005). However, it cannot handle multiple bounce events.

Alternatively, we can solve a conventional dip limited one-way WE algorithm in a tilted co-ordinate reference frame. A sum over migration components run in several tilted frames can successfully image turning wave arrivals (Shan & Biondi, 2004).

Using RTM, which we consider here, we have a full solution to the acoustic two-way wave equation. The version used in the case study shown here involved an 8th order solution in space, and incorporated polar anisotropy with a vertical symmetry axis (VTI) (Zhou, 2006). RTM has the potential to migrate all multiples, although some consideration must be given to the boundary conditions. Although the theory dictates that recordings should be made on two (horizontal) levels, rather than the single recording level that we usually have at the earth's surface (Mittet, 2006),

practise shows that multiples can be profitably handled, giving enhanced images of the subsurface. This may be of particular use for VSP imaging.

However, in order to image multiples, we would need a very detailed and accurate representation of the velocity contrasts associated with them, in our model (i.e. the model would need to include all interfaces that generated significant multiple reflection energy). Such detail is not always possible (or practical) to achieve: consequently, we still strive to suppress multiple energy in the pre-processing.

To demonstrate the potential of RTM to image complex bodies, we first consider a complex isotropic acoustic FD synthetic data example (courtesy of BP, first shown at the EAGE Paris model building workshop: Billette & Brandsburg-Dahl, 2005). In figure 1, we have the result for a one-way WE, and in figure 2, the result from RTM. In the one-way image, we are unable to handle turning ray energy that illuminates the overhanging salt, and the steep portions of the salt stems are either not imaged (due to algorithmic dip limitation) or not illuminated by the acquisition. Steep dips, and the turning wave energy, as well as energy from other two-way ray paths, are handled by the RTM, producing a good image. The one-way migration examples shown in this paper were obtained using a split-step Fourier plus interpolation algorithm (SSFPI).

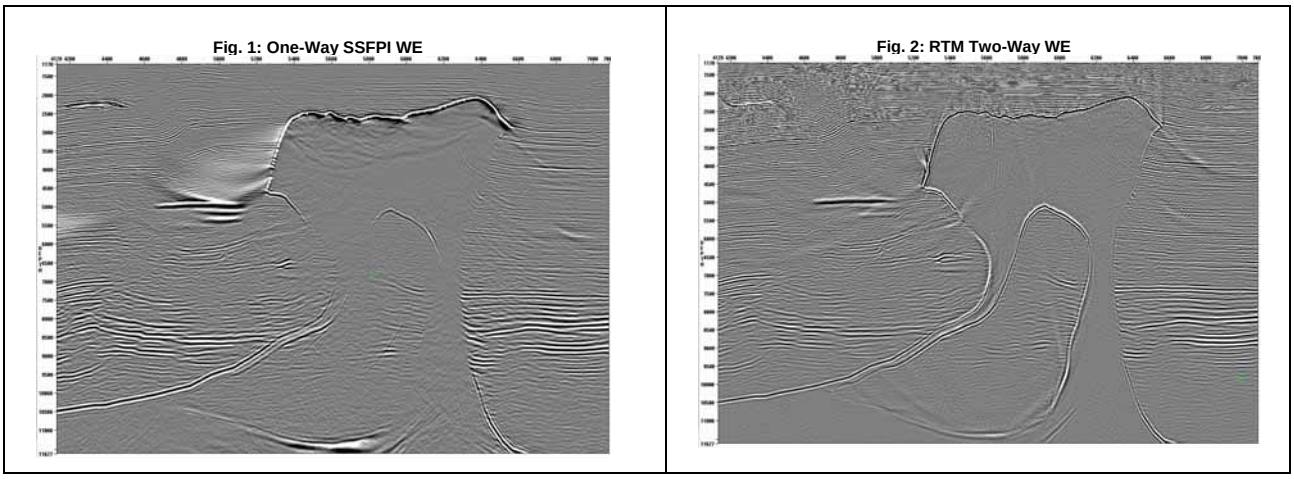

Figure 1. A subsalt image generated with an SSFPI one-way WE migration shows poor imaging of salt flanks and subsalt structures. Figure 2. A subsalt image generated with RTM technology shows significant improvement in imaging salt flanks, even beneath the salt. (input synthetic data courtesy of BP, imaging by GXT)

Results

The North Sea data considered here (Jones, et al, 2006) show one of the classic mushroom shaped salt domes typical of parts of the North Sea. The otherwise flat-lying chalk beds are upturned during deposition as the salt piercement continues contemporaneously with sediment deposition (Davison et al, 2000, Thomson, 2004). A commercial WE project had recently been completed, so we had a 'final' model available (figure 4), as well as comparisons of the usual one-way WE and Kirchhoff images. For example, figure 4 shows a Kirchhoff preSTM result, where a base-salt event is visible.

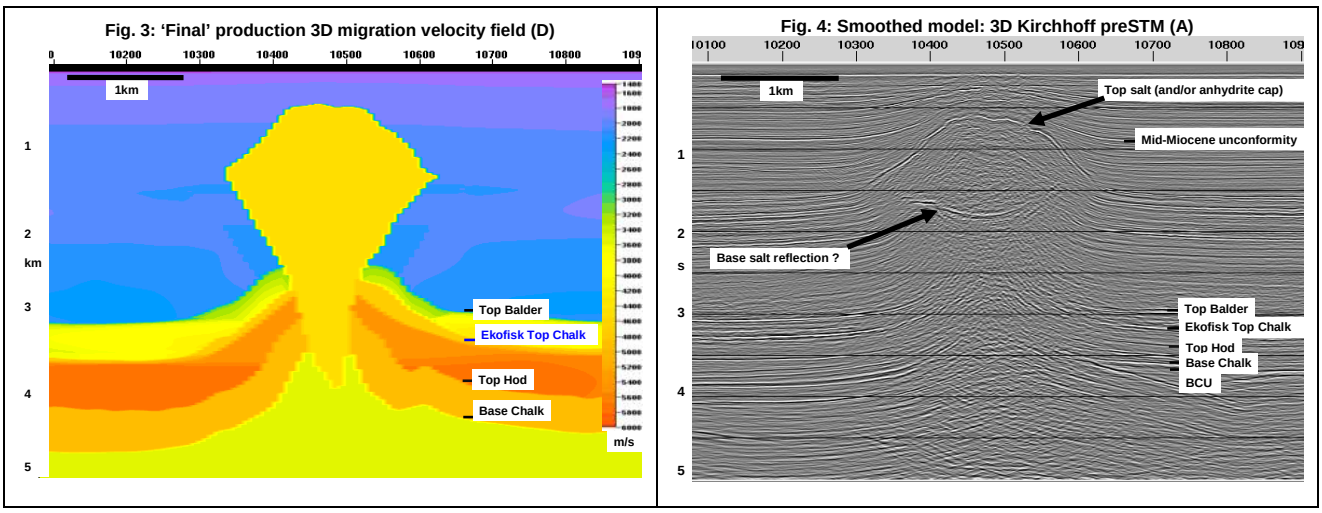

Figure 3) 'Final' production model for line D. Figure 4, Kirchhoff preSTM for a near-crestal line (A), showing clear base-salt refection energy.

As with any complex data, or in trying to understand the kinematics of a new algorithm, forward modelling tests are often instructive. With this in-mind, we ran some 2D ray-tracing through a model of a crestal line from this salt body. Our main interest with this was to ascertain what classes of energy may be involved in illuminating the steep salt flank events. In figure 5a we show the ray trace results for events passing through the top salt, propagating as P waves, and illuminating the salt flanks. Figure 5b shows the corresponding ray paths for the PSSP arrivals. In figure 5c we show ray paths for prism waves (double bounces) that reflect of both the salt flanks and the flat lying top Balder and top Chalk events. The predominant class of energy illuminating the salt flank seems to be the prism wave arrivals. In this case we were not able to unambiguously identify PSSP arrivals in the real data (although we make some comment on this class of arrival later).

Turning-ray energy was not present for these data, as the vertical velocity gradients in the overburden were slight, and included a significant velocity inversion at the mid-Miocene unconformity.

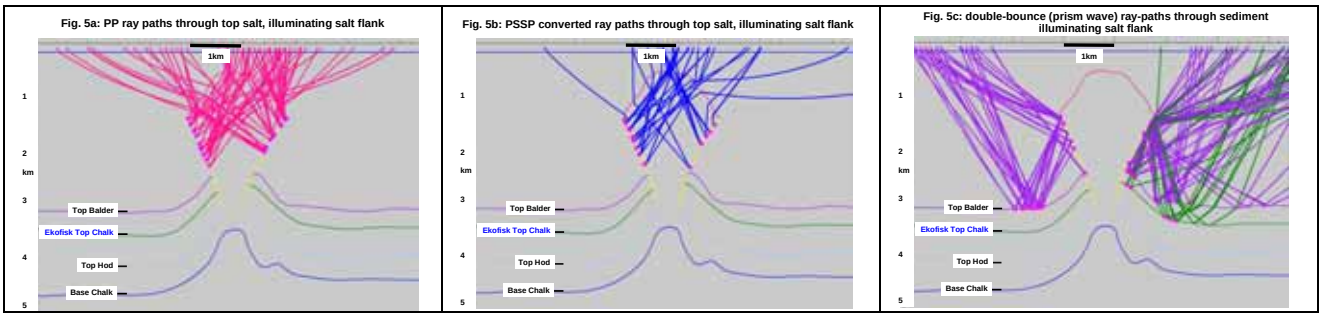

Figure 5: a) PP ray paths through top salt; b) PSSP ray paths; c) prism wave energy illuminating steep flanks of structure.

Using this conventionally derived final model, we ran an RTM, limiting the modelling frequency to 17Hz. The results of the RTM clearly indicated the inadequacies of the conventional model building route, and we proceeded to attempt to refine the model based on iterative RTM model update. Figures 6, 7, 8, and 9 show respectively a Kirchhoff preSDM, a WE preSDM, another line from the WE preSDM after high-cut filtering to resemble the RTM bandwidth, and an RTM using the 'final' model from the commercial project. It should be noted that as these images were archived during different stages of a now completed commercial project, that they differ slightly in terms of input and output trace spacing, wavelet processing, and final bandwidth. However, these differences will not have an impact on the conclusions drawn here.

We see from the RTM that we have very steep salt flank arrivals (perhaps from an upturned chalk interface). From the ray-trace study, it is likely that these steep events come from prism wave illumination. The salt interpretation in this model, made on the basis of the WE results, looks like it is incorrect near the edges of the salt, especially on the right hand side (a salt proximity study was used to constrain the model to the left of the salt body, as seen in these images). The RTM result indicates that the salt is probably a bit less wide, with near-vertical edges below a slight overhang. Also, the RTM result indicates that the top Balder and top Chalk events probably turn-up sharply to abut the salt, rather than 'rolling through' the model with a gentle anticlinal shape, as was used in the production model.

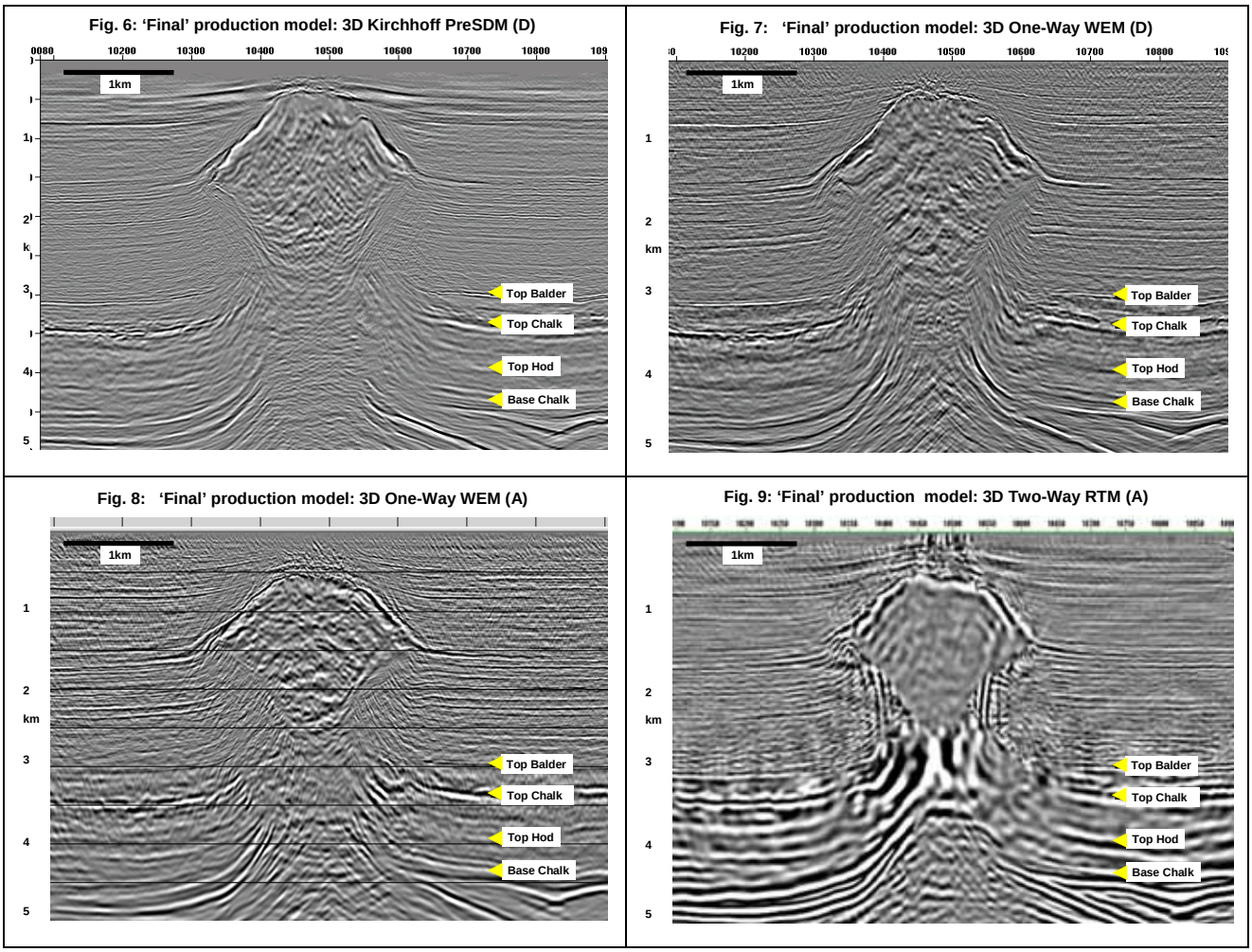

Figure 6, Kirchhoff preSDM for line D. Figure 7, SSFPI WE preSDM for line D. Figure 8, low-pass filtered SSFPI WE preSDM from line A. Figure 9, RTM for line A. All five figures here have used the 'final' production 3D model.

Two sediment flood models were then employed to assess the potential of the RTM imaging for model update. The first was a sediment-only model (figure 10a) with only the moderate shallow velocities present (no top balder or top chalk, etc). The second flood model contained the top Balder (the first major velocity increase) and the subsequent chalk layers. The geometry of these high velocity layers below the position of the (absent) salt, was left as a gentle anticline (figure 11a).

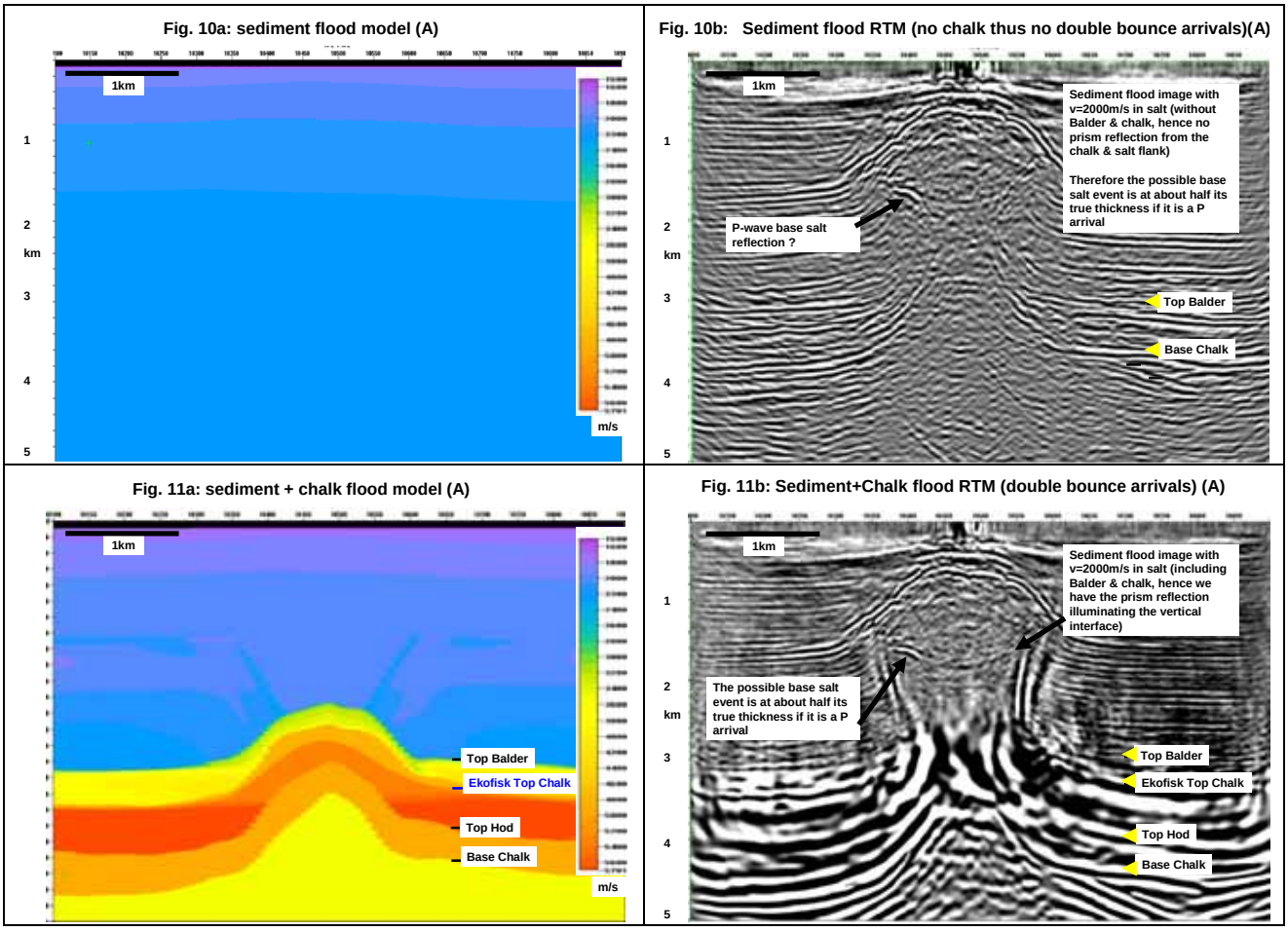

Figure 10a: sediment-only flood model for line A. Figure 10b: sediment-only flood RTM for line A. Figure 11a, sediment + chalk flood model for line A. Figure 11b, sediment + chalk flood RTM for line A.

In the 'sediment only' flood RTM result (figure 10b) we see a good top salt image, but no steep events. The steep events, interpreted to be prism wave reflections, are absent in these data because the velocity model does not include the flat lying top Balder or top Chalk events which are required to generate one side of the double bounce. However in the 'sediment+chalk' flood RTM result (figure 11b), we clearly see these steep events. This is a clear indication that the steep events are prism wave arrivals, incorporating a bounce from the flat lying top Balder and/or Chalk horizons, and then reflecting from the steep salt (or sediment) flanks.

Such sediment floods will help delineate the steep events with ray paths that travelled through the sediments only (as shown in the ray tracing of figure 5c). For ray paths that travel through the salt (as per figure 5a) we would need a salt flood. This was performed; however, for the most-part, no clear base salt was visible. This may indicate that our top salt pick is not accurate enough. It is also known that this salt dome has an anhydrite cap rock of variable thickness and high velocity (~6000m/s). This was not incorporated in the model, as we were unable to pick it: this too may contribute to the poor imaging of the base salt. We know that base salt reflection energy is present in the input data, as it is visible in a preSTM (figure 4), and the sediment flood RTM results. Figure 12a shows the salt flood RTM result for line C, which shows a possible base salt reflection. The salt-flood model has salt throughout the model below the mid-Miocene unconformity. Figure 12b shows 'sediment+chalk' flood RTM result for line C for comparison. If the 'base salt' event in the salt-flood is PP energy, then this event should appear at about half its thickness in the corresponding sediment flood results (note that whereas the salt flood velocity was 4500m/s, the sediment flood velocity in the salt region was only 2000m/s, and not half the salt velocity).

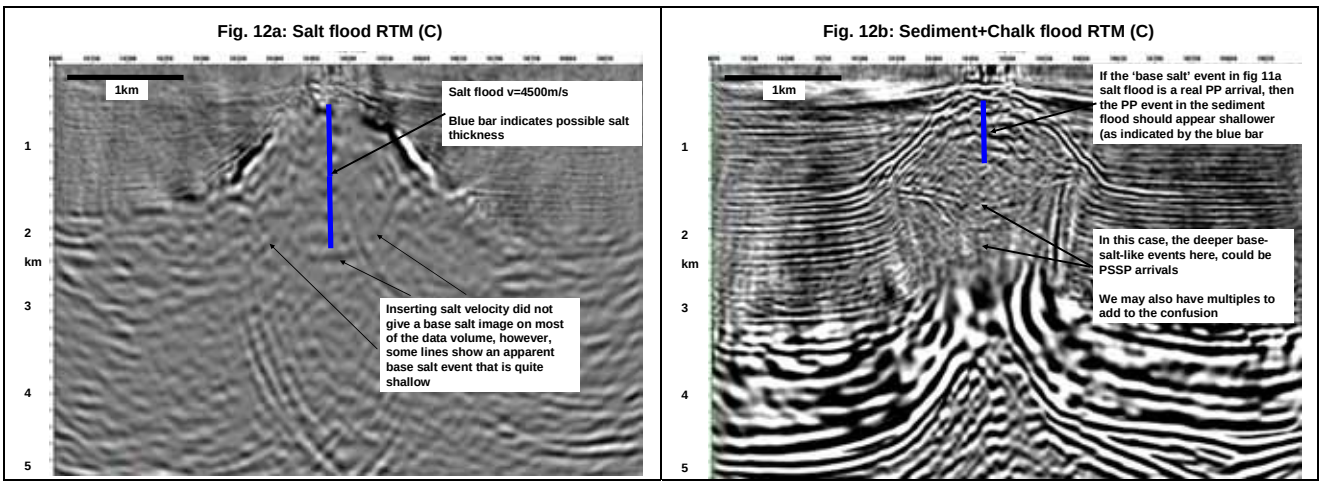

Figure 12a, salt-flood RTM for line C. Figure 12b, 'sediment + chalk' flood RTM for line C. The event in a) which could be a base-salt PP arrival should appear at about half the salt thickness in the 'sediment+chalk' flood image b). The blue bar represents the interpreted salt thickness on a), and the corresponding predicted salt thickness for b).

For real data from complex salt provinces, we often see images of converted mode energy (PSSP) in our P-wave images. This energy has usually undergone P to S conversion at the top salt interface, propagates through the salt as S, reflecting at the base salt, and then converts back to P at the top salt to be recorded in our hydrophone streamer data (figure 5b). It is interesting to note that we can even observe converted mode energy at zero offset, due to the triangular geometry of some salt bodies (Lafond, et al, 2003). For acoustic imaging, such arrivals constitute a pernicious class of noise, as the events can be mistaken for the P wave base salt reflections. For the real data considered here, we have various reflections from the base salt, some of which could be converted modes (as indicated on figure 12b). Consequently, it is important to recognize them, as such arrivals can easily confuse an interpreter during model building. Occasionally we can make use of them to help delineate the base salt events (Lewis, 2006).

Conclusions

Complex bodies such as salt domes are illuminated by many wave paths that cannot be imaged by conventional one-way propagators. Significant improvement can be achieved both in the model building and final migration by employing a two-way wave equation migration scheme.

The first of these points is perhaps the most significant: if we cannot derive an accurate velocity model of the subsurface, then our final imaging step will not produce a reliable image.

It is the combination of model building and migration that is the key to successful imaging. We have shown in this work that iterative application of RTM can help delineate the correct salt geometry, whereas a one-way method failed to do so.

Subsequent imaging of the salt body shows enhancements to steep and overturned flanks, most likely illuminated by prism waves (double bounce arrivals). Errors in the velocity and anisotropy parameters will greatly influence the positions of near-vertical events, so misalignment of the vertical salt (or sediment) flanks seen here could be used to assist with model update.

Acknowledgements

We wish to thank BP for providing the complex salt synthetic data. Our thanks also to Ivan Berranger, Debashish Sarkar, Brent Mecham, and Mick Sugrue at GX Technology for help

preparing examples, and for useful discussion. The authors wish to thank the management of GX Technology and its parent company, Input/Output, for permission to publish the results of this study.

References

Baysal, E., Kosloff, D. D. and Sherwood, J. W. C., 1983, Reverse time migration: GEOPHYSICS, Soc. of Expl. Geophys., 48, 1514-1524.

Bednar, J.B., Yoon, K., Shin, C. and Lines, L. R., 2003, One Way vs Two Way Wave Equation Imaging – Is Two-Way Worth It?, 65th Mtg.: Eur. Assn. Geosci. Eng., B11

Bernitsas, N., Sun, J., & Sicking, C., 1997: Prism waves – an explanation for curved seismic horizons below the edge of salt bodies, 59th Ann. Internat. Mtg. Europ. Assoc. Expl. Geophys.

Billette, F.J., and S. Brandsberg-Dahl, 2005, The 2004 BP Velocity Benchmark: 67th Meeting, Eur. Assn. Geosci. Eng., Expanded Abstracts, B035

Cavalca, M., & Lailly, P., 2005, Prismatic reflections for the delineation of salt bodies, 75th Ann. Internat. Mtg: Soc. of Expl. Geophys.

Davison, I., Alsop, G.I., Evans, N.G., Safaricz, M., 2000, Overburden deformation patterns and mechanisms of salt diaper penetration in the Central Graben, North Sea. Marine and Petroleum Geology, 17, p601-618.

Diet, J. P. & Lailly, P., 1984, Choice of scheme and parameters for optimal finite-difference migration in 2-D, 54th Ann. Internat. Mtg: Soc. of Expl. Geophys.

Farmer, P., 2006, Back to the future: New advances in reverse time migration provide sub-salt imaging solutions, Hart's E&P, May 2006

Jones, I.F., 1992, Comparative anatomy of 3D one-pass depth migration schemes: 62nd annual meeting of the Society of Exploration Geophysicists

Jones, I.F. & Lambaré, G. 2003, Wave equation versus ray based imaging. First Break, v21, No.2, pp11-13.

Jones, I.F., Sugrue, M. King, D., Goodwin, M., Berranger, I., Zhou, H., Farmer, P., 2006, Application of reverse time migration to complex North Sea imaging, PETEX bi-ennial meeting.

Jones, I.F., Bloor, R.I., Biondi, B., Etgen J.T., 2006, Pre-stack depth migration and velocity model building, SEG Geophysical Reprints, Series Editor: Michael A. Pelissier, in press

Lafond, C., Jones, I.F., Bridson, M., Houllevigue, H., Kerdraon, Y., & Peliganga, J.,2003, Imaging Deep Water Salt Bodies in West Africa, The Leading Edge, v22, No.9, pp893-896.

Lewis, J., 2006, The potential of mode-converted waves in salt interpretation. SEG/EAGE summer research workshop, Utah.

Mittet, R., 2006, The behaviour of multiples in reverse time migration, 68th Ann. Internat. Mtg. Eur. Assn. Geosci. Eng.,

Pelissier, M.A., Hoeber, H., van de Coevering, N., Jones, I.F., 2006, Classics of Elastic Wave Theory, SEG Geophysical Reprints, Series Editor: Daniel A. Ebrom, in press

Shan, G., and B. Biondi, 2004, Imaging overturned waves by plane wave migration in tilted co-ordinates: 74th Annual International Meeting, SEG, Expanded Abstracts, 969-972.

Thomson, K., 2004, Overburden deformation associated with halokinesis in the Southern North Sea: implications for the origin of the Silverpit Crater. Vis Geosci, 9, p1-9.

Whitmore, N. D., 1983, Iterative depth migration by backward time propagation: 53rd Annual International Meeting, SEG, Expanded Abstracts, Session:S10.1.

Yoon, K., Shin, C., Suh, S., Lines, L. R. and Hong, S., 2003, 3D reverse-time migration using the acoustic wave equation: An experience with the SEG/EAGE data set: THE LEADING EDGE, 22, no. 1, 38-41

Zhou, H., Zhang, G., Bloor, R., 2006, Anisotropic Acoustic Wave Equation for VTI Media, 68th Ann. Internat. Mtg. Eur. Assn. Geosci. Eng.,

Zhang, Y., Sheng, X., Zhang, G., 2006, Imaging complex salt bodies with turning-wave one-way wave equation. SEG/EAGE summer research workshop, Utah.